

Cascade Control Approach for a Cart Inverted Pendulum System Using Controller Synthesis Method *

Fuat Peker, Ibrahim Kaya, Erdal Cokmez and Serdal Atic

Abstract— Inverted pendulum is a basic benchmark in the field of control engineering. It is a well-known example of single input multi output (SIMO) systems. A commonly used type of the inverted pendulum systems is cart inverted pendulum which has a cascade structure inherently. In this paper, a cascade control approach based on controller synthesis method is used for controlling a cart inverted pendulum system. Controller synthesis technique is used to tune both inner and outer loops of the cascade control system. Simulation results are given to demonstrate the use of the proposed approach.

I. INTRODUCTION

Looking at the areas of control engineering and robotics, there are many systems that have been used to test new developed control techniques or used for training purposes. Among these, inverted pendulum is one of the most known and widely used. It is a good example of under actuated mechanical systems (UMS). These systems are frequently handled in the robotics area. Fundamental property of the UMS is that they have more degree of freedom than number of actuators [1]. Inverted pendulum is a highly nonlinear and unstable system. Because of this structure, it attracts great interest from researchers and is often used in the studies related to control theory. Another important property of the inverted pendulum is that it creates sub models for many systems used today. For instance; humanoid robots, seismographs, single-link robot arm, automatic aircraft landing system, attitude control of a space booster rocket and a satellite and etc [2].

When looking at control engineering and robotics fields, various types of inverted pendulum are encountered. The most known inverted pendulum types are cart inverted pendulum [3], double inverted pendulum [4] and rotational single arm pendulum (Furuta pendulum) [5]. In this study cart inverted pendulum type is used.

There are many studies in the literature intended for control of the inverted pendulum. Some of the studies are about bringing the pendulum from downward stable position to upward unstable position by swinging. However, most of the studies related to inverted pendulum are about

stabilization of the pendulum in unstable upright position. Linear methods such as proportional-integral-derivative (PID) controller and linear quadratic regulator (LQR) are used for controlling the inverted pendulum system. The study given in [6], two PID controllers designed by stability boundary locus method are used to control a cart inverted pendulum system. In [7], an LQR controller is used in the state feedback along with PID controller to control an inverted pendulum system. In this study, ant colony optimization (ANO) technique is used to tune both PID controller and LQR state feedback controller. Two fractional order PID controllers, which are designed by particle swarm optimization (PSO) method, are proposed in [8] to robustly control a cart inverted pendulum system. Some nonlinear control approaches such as sliding mode control (SMC) and backstepping control are also used for control of the inverted pendulum system. In [9], a SMC is proposed to balance a cart inverted pendulum system. A second order SMC is used to control a cart inverted pendulum system in [10]. A robust adaptive backstepping controller is proposed in [11] to stabilize an inverted pendulum on a cart. Intelligent control methods such as adaptive neuro fuzzy inference system (ANFIS) and artificial neural network (ANN) and hybrid control approaches created by combining different methods are other control techniques used to control the inverted pendulum system. One can look at the studies given in [12]–[14] to see the intelligent control approaches applied to the inverted pendulum system.

From above examples it is seen that many control methods have been applied to the inverted pendulum system. In the linear methods (especially based on PID controllers), to the authors' knowledge, most of the studies use two separate controllers to control the cart inverted pendulum system. In these studies, one of the controllers is designed for pendulum angle and the other is designed for cart position separately. After the controllers are designed, they are combined in a control strategy given in Fig. 1. However, the control strategy given in Fig. 1 is not considered as a good method due to inherent cascade structure of the cart inverted pendulum system. Therefore, in this paper an improved cascade control approach has been proposed to control a cart inverted pendulum system. Tuning parameters of controllers have been determined by using controller synthesis method [15].

The rest of the paper is organized as follows. In section 2, the cart inverted pendulum system is introduced and modeling of the system is given. The cascade control strategy of the cart inverted pendulum system is explained in section 3. In section 4, simulation results belong to given approach are provided. Conclusions are included in section 5.

*Research supported by Dicle University Coordinatorship of Scientific Research Projects (DUBAP).

F. Peker is with the Department of Electrical-Electronics Engineering Dicle University, 21280 Diyarbakir, TURKEY (phone: +90-412-241-1010 (3639); e-mail: fuat.peker@dicle.edu.tr).

I. Kaya is with the Department of Electrical-Electronics Engineering, Dicle University, 21280 Diyarbakir, TURKEY (e-mail: ikaya@dicle.edu.tr).

E. Cokmez is with the Department of Electrical-Electronics Engineering, Dicle University, 21280 Diyarbakir, TURKEY (e-mail: erdal.cokmez@dicle.edu.tr).

S. Atic is with the Department of Electric and Energy, Batman University, 72060 Batman, TURKEY (e-mail: serdal.atic@batman.edu.tr).

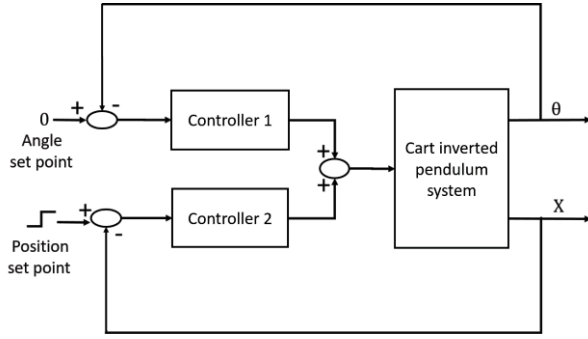


Figure 1. Control strategy obtained by combining two separate controllers for cart inverted pendulum system

II. CART INVERTED PENDULUM SYSTEM

Cart pendulum structure is formed from a cart and a pendulum attached on it shown in Fig 2. The pendulum in the cart pendulum system has two equilibrium points: one is stable and the other is unstable. The stable equilibrium point is the downward equilibrium point where the pendulum finally reaches after it is released or exposed by a force. The unstable equilibrium point is the vertical upward point where the pendulum cannot be balanced without applying a control force. The cart inverted pendulum is the system obtained by balancing the pendulum in the unstable upright position. The cart inverted pendulum system is a single-input multi-output (SIMO) system. The single input of the system is the force applied to the cart and the outputs of the system are pendulum angle and cart position. By applying the appropriate force to the cart, stabilizing of the inverted pendulum (pendulum in the unstable upright position) and cart position control can simultaneously be achieved.

The following nonlinear equations of motion can be obtained by using the forces and moments acting on the pendulum and the cart shown in Fig. 2.

$$(M + m)\ddot{x} + b\dot{x} + ml\ddot{\theta}\cos(\theta) - ml\dot{\theta}^2\sin(\theta) = F \quad (1)$$

$$(I + ml^2)\ddot{\theta} - mgl\sin(\theta) + ml\ddot{x}\cos(\theta) = 0 \quad (2)$$

The values of the parameters in (1) and (2) are given in Table I. These values are taken from the cart pendulum setup manufactured by Feedback Instruments Ltd [16].

TABLE I. VALUES OF PARAMETERS

| Parameter | Value |
|-------------------------------------|-------------------------|
| g – gravity | 9.81 m/s ² |
| M – cart mass | 2.4 kg |
| m – pendulum mass | 0.46 kg |
| l – pendulum length | 0.36 m |
| I – moment of inertia of pendulum | 0.099 kg.m ² |
| b – cart friction coefficient | 0.05 N.s/m |

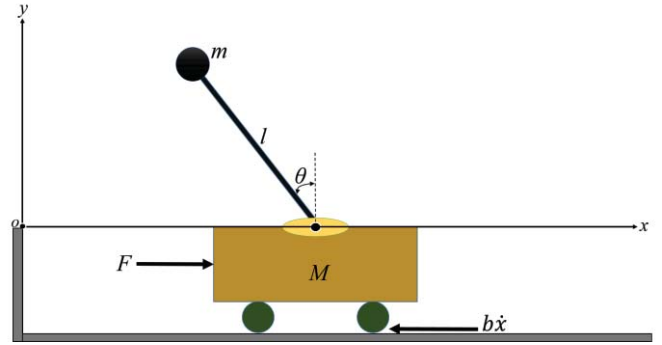


Figure 2. Cart pendulum structure

In the cart inverted pendulum system, the unstable equilibrium point is the point where the pendulum angle (θ) is 0 rad. For small angle deviations around $\theta = 0$ rad, following assumptions can be made.

$$\theta \approx 0 \Rightarrow \cos(\theta) \approx 1, \sin(\theta) \approx \theta, \dot{\theta}^2 \approx 0 \quad (3)$$

According to assumptions in (3), the nonlinear equations given in (1) and (2) can be linearized as follows.

$$(M + m)\ddot{x} + b\dot{x} + ml\ddot{\theta} = F \quad (4)$$

$$(I + ml^2)\ddot{\theta} - mgl\theta + ml\ddot{x} = 0 \quad (5)$$

The cart friction coefficient (b) is very small in comparison to other parameters. So, it can be neglected. After taking Laplace transform of (4) and (5) and substituting values of the parameters, the following transfer functions are obtained.

$$\frac{\theta(s)}{F(s)} = \frac{ml}{\left[(ml)^2 - (M + m)(I + ml^2)\right]s^2 + (M + m)mgl} \quad (6)$$

$$\frac{X(s)}{\theta(s)} = -\frac{(I + ml^2)s^2 - mgl}{mls^2} \quad (7)$$

The constants in (6) and (7) are $K_1 = 0.0356$, $T_1 = 0.3029$, $K_2 = 9.8098$ and $T_2 = 0.3124$. As can be clearly seen from (6) and (7), the cart inverted pendulum system has a cascade structure shown in Fig. 3.

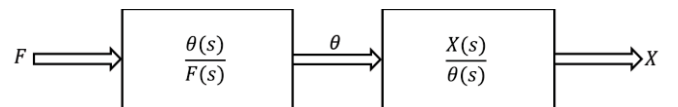


Figure 3. Cascade structure of the cart inverted pendulum system

III. CASCADE CONTROL DESIGN

Cascade control approach proposed in this paper to control the cart inverted pendulum system is given in Fig. 4. In this control strategy, there are two processes to be controlled: inner process ($G_1(s)$) and outer process ($G_2(s)$). There are two controllers to be designed: inner loop controller ($C_1(s)$) and outer loop controller ($C_2(s)$).

The inner loop controller is necessary to stabilize the pendulum in the unstable upright (inverted) position. As it is seen from (6), transfer function for the pendulum angle is a second order unstable one. In the control strategy given in Fig. 4, before designing the inner loop controller, it is considered that the inner process should be stabilized to control it more efficiently. For this purpose, a proportional-derivative (PD) block ($PD_1(s)$) is placed in the inner feedback loop containing $G_1(s)$ as shown in Fig. 4. Transfer function of the $PD_1(s)$ is given by

$$PD_1(s) = K_{f1} + K_{d1}s. \quad (8)$$

By adding $PD_1(s)$ in the inner feedback loop containing $G_1(s)$, the closed loop transfer function $T_{ii}(s)$ is obtained as given below.

$$T_{ii}(s) = \frac{-0.0356}{0.0917s^2 - 0.0356K_{d1}s - 0.0356K_{f1} - 1} \quad (9)$$

To make $T_{ii}(s)$ stable, following intervals are found for K_{f1} and K_{d1} by using the Routh–Hurwitz stability criterion.

$$K_{f1} < -28.0899, \quad K_{d1} < 0 \quad (10)$$

According to intervals given in (10), values are selected as $K_{f1} = -33$ and $K_{d1} = -3$. Now, the inner loop controller ($C_1(s)$) can be designed for the stabilized $T_{ii}(s)$. The controller synthesis method can be applied by assuming that the closed loop transfer function is similar to the first order or second order transfer function [15]. From Fig. 4, the inner closed loop transfer function can be derived as

$$\frac{\theta(s)}{R_1(s)} = \frac{C_1(s)T_{ii}(s)}{1 + C_1(s)T_{ii}(s)}. \quad (11)$$

The inner loop controller can be calculated from (11) as follows.

$$C_1(s) = \frac{\theta(s) / R_1(s)}{T_{ii}(s)[1 - \theta(s) / R_1(s)]} \quad (12)$$

The inner closed loop response is assumed to be similar to response of the first order process transfer function given in the following [15].

$$\frac{\theta(s)}{R_1(s)} = \frac{1}{\tau_c s + 1} \quad (13)$$

In (13), τ_c is the inner closed loop time constant defined by user. By substituting (9) and (13) in (12), following transfer function for the $C_1(s)$ is calculated.

$$C_1(s) = \frac{-3}{\tau_c} + \frac{-4.9101}{\tau_c} \frac{1}{s} + \frac{-2.5772}{\tau_c} s \quad (14)$$

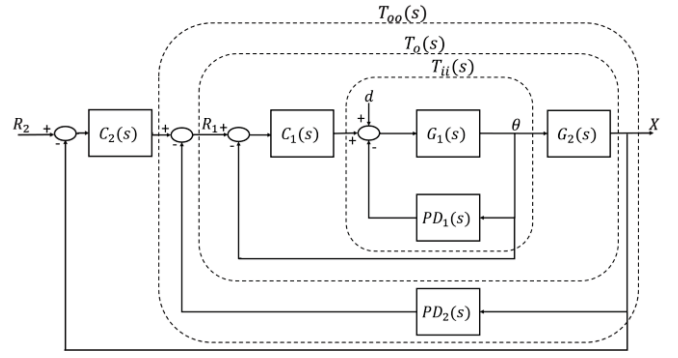


Figure 4. Cascade control approach

It is obviously seen that $C_1(s)$ is an actual PID controller and tuning parameters of which are given as

$$K_{pi} = \frac{-3}{\tau_c}, \quad K_{ii} = \frac{-4.9101}{\tau_c}, \quad K_{di} = \frac{-2.5772}{\tau_c}. \quad (15)$$

From (15), it is seen that the inner loop controller parameters only depend on inner closed loop time constant τ_c .

The outer loop controller ($C_2(s)$) is for the position control of the cart. In the cascade control approach given in Fig. 4, transfer function for the cart position control ($T_o(s)$) is obtained by multiplying inner closed loop transfer function with the outer process ($G_2(s)$). $T_o(s)$ is given as

$$T_o(s) = \frac{K_2(1 - T_2s)(1 + T_2s)}{s^2(\tau_c s + 1)}. \quad (16)$$

$T_o(s)$ have double integrators. So, like for the inner process, a PD ($PD_2(s)$) block is located in the inner feedback loop containing $T_o(s)$ as shown in Fig. 4 to make it stable. Transfer function of the $PD_2(s)$ is given as follows.

$$PD_2(s) = K_{f2} + K_{d2}s \quad (17)$$

The closed loop transfer function $T_{oo}(s)$ is obtained by adding $PD_2(s)$ in the inner feedback loop containing $T_o(s)$ as follows.

$$T_{oo}(s) = \frac{9.8098(1 - 0.3124s)(1 + 0.3124s)}{(\tau_c - 0.9574K_{d2})s^3 + (1 - 0.9574K_{f2})s^2 + 9.8098K_{d2}s + 9.8098K_{f2}} \quad (18)$$

The Routh–Hurwitz stability criterion is used to make $T_{oo}(s)$ stable and intervals for K_{f2} and K_{d2} are found as

$$0 < K_{f2} < 1.0445, \quad K_{f2}\tau_c < K_{d2} < 1.0445\tau_c. \quad (19)$$

Values of K_{f2} and K_{d2} are chosen as midpoints of the intervals given in (19). So, although value of K_{f2} is selected as a constant of 0.5222, value of K_{d2} can change according to inner closed loop time constant τ_c . From Fig. 4, the outer closed loop transfer function can be obtained as follows.

$$\frac{X(s)}{R_2(s)} = \frac{C_2(s)T_{oo}(s)}{1 + C_2(s)T_{oo}(s)} \quad (20)$$

The outer loop controller can be derived from (20) as follows.

$$C_2(s) = \frac{X(s) / R_2(s)}{T_{oo}(s)[1 - X(s) / R_2(s)]} \quad (21)$$

The outer closed loop response is assumed to be similar to response of the second order process transfer function given as [15]

$$\frac{X(s)}{R_2(s)} = \frac{\omega_n^2 (1 - T_2 s)}{s^2 + 2\zeta\omega_n s + \omega_n^2}. \quad (22)$$

Here, ω_n and ζ are natural frequency and damping ratio, respectively which are defined by user. By substituting (18) and (22) in (21), following transfer function for the $C_2(s)$ is obtained.

$$C_2(s) = \frac{\omega_n^2 [As^3 + Bs^2 + Cs + D]}{9.8098s(1 + 0.3124s)((2\zeta\omega_n + 0.3124\omega_n^2) + s)} \quad (23)$$

Here, A , B , C and D are given as

$$\begin{aligned} A &= (\tau_c - 0.9574K_{d2}), & B &= (1 - 0.9574K_{f2}), \\ C &= 9.8098K_{d2}, & D &= 9.8098K_{f2}. \end{aligned} \quad (24)$$

Assuming that s_1 , s_2 and s_3 are roots of the polynomial equation $As^3 + Bs^2 + Cs + D = 0$, then $C_2(s)$ can be written as

$$C_2(s) = \left[\frac{s - s_1}{(1 + 0.3124s)((2\zeta\omega_n + 0.3124\omega_n^2) + s)} \right] \left[\left(\frac{\omega_n^2}{9.8098} \right) \left(\frac{s^2 - (s_2 + s_3)s + s_2s_3}{s} \right) \right] \quad (25)$$

The first term

$$\left[\frac{s - s_1}{(1 + 0.3124s)((2\zeta\omega_n + 0.3124\omega_n^2) + s)} \right] \quad (26)$$

is considered as a noise filter. The second term

$$\left[\left(\frac{\omega_n^2}{9.8098} \right) \left(\frac{s^2 - (s_2 + s_3)s + s_2s_3}{s} \right) \right] \quad (27)$$

is the transfer function of an actual PID controller and tuning parameters of which are given as

$$\begin{aligned} K_{po} &= \frac{-\omega_n^2}{9.8098}(s_2 + s_3), \\ K_{io} &= \frac{\omega_n^2}{9.8098}(s_2s_3), \\ K_{do} &= \frac{\omega_n^2}{9.8098}. \end{aligned} \quad (28)$$

Consequently, the outer loop controller $C_2(s)$ is obtained as a PID controller with a noise filter term. Since τ_c , K_{f2} and K_{d2} are designated before, it is seen from (23) and (24) that $C_2(s)$ depends on damping ratio and natural frequency which are defined by user.

Choosing values of the damping ratio ζ and the inner closed loop time constant τ_c can be done easily. But, choosing a value for the natural frequency ω_n is not easy [15]. So, the method used in [15] which is given below are also used here to determine the natural frequency value.

$$\omega_n = \frac{2.5}{\zeta T_s} \quad (29)$$

Here, T_s is the settling time specified by user. So, there are only three parameters, τ_c , ζ and T_s , defined by user.

IV. RESULTS

In this section, simulation results of the cascade control approach given in Fig. 4 to control the cart inverted pendulum system is provided. Performance of the given approach is analyzed according to changing values of inner closed loop time constant τ_c , damping ratio ζ and settling time T_s .

To examine the performance of the system, a disturbance amplitude of which is -0.5 is applied to the system at time $t = 25$ second from disturbance input d shown in Fig. 4. Then, at time $t = 50$ second, a pulse signal is applied to the system from input R_2 as a reference trajectory for the cart. Amplitude and period of pulse signal are 0.5 m and 50 seconds, respectively. Responses of the system for changing values of inner closed loop time constant τ_c , damping ratio ζ and settling time T_s are given in Fig. 5, Fig. 6 and Fig. 7, respectively. The upper figures show pendulum angle responses and the lower figures show cart position responses.

For the responses demonstrated in Fig. 5, damping ratio ζ and settling time T_s are taken as 0.9 and 1 second, respectively. Values of inner closed loop time constant τ_c are changed from 0.1 to 0.7. It is seen from Fig. 5 that both pendulum angle and cart position responses of the system are affected negatively in terms of maximum overshoot and oscillations while τ_c is increasing. If τ_c is increasing much, pendulum may fall and hence, the system may breaks down. As shown in Fig. 5, it is also should be noted that disturbance rejection performance of the system is also negatively affected with the increasing value of τ_c .

Responses of the system for changing damping ratio ζ are illustrated in Fig. 6. Here, values of inner closed loop time constant τ_c and settling time T_s are fixed as 0.1 second and 1 second, respectively. From Fig. 6, both pendulum angle and cart position responses of the system have smaller overshoots and less oscillation with the increasing value of ζ as expected.

In Fig. 7, system responses according to changing values of settling time T_s are given. Inner closed loop time constant τ_c and damping ratio ζ have fixed values of 0.1 second and 0.95, respectively. When analyzing Fig. 7, it is seen that unlike the increasing τ_c case, both outputs of the system have smaller overshoot and less oscillations with the increasing T_s value

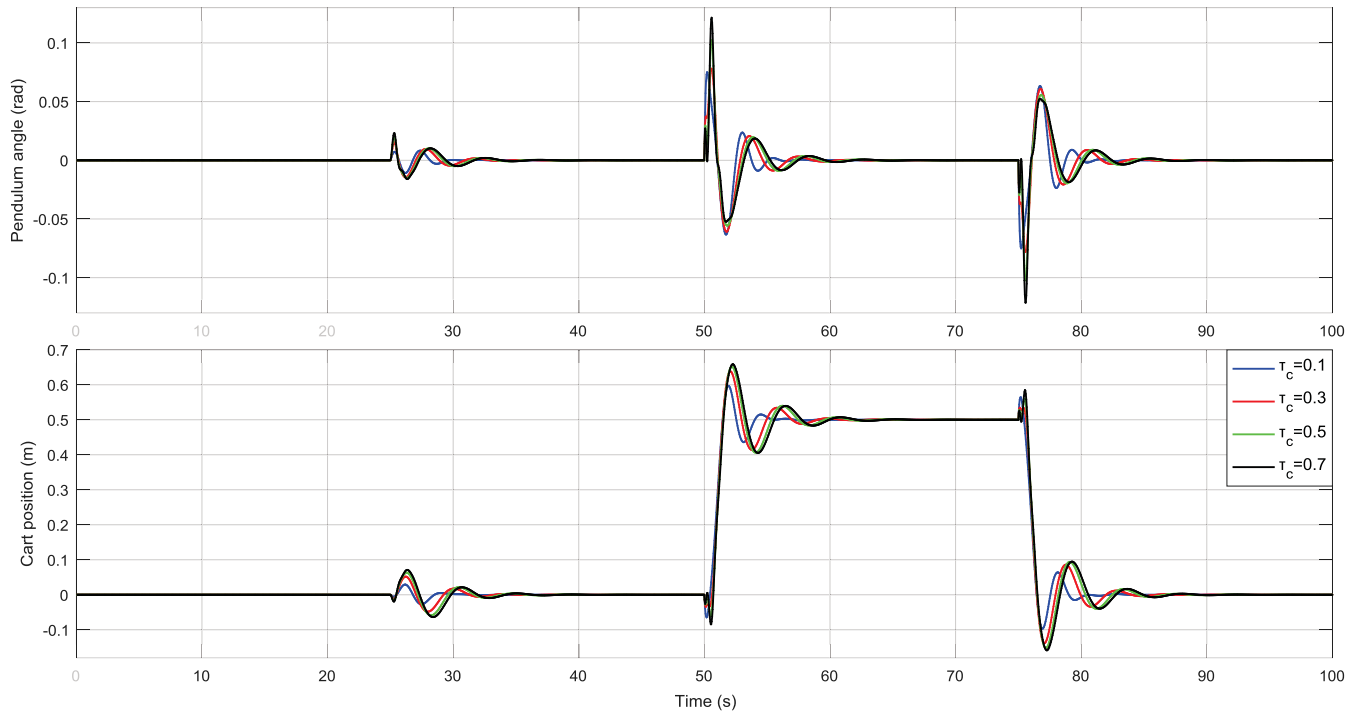


Figure 5. Responses for changing values of inner closed loop time constant τ_c

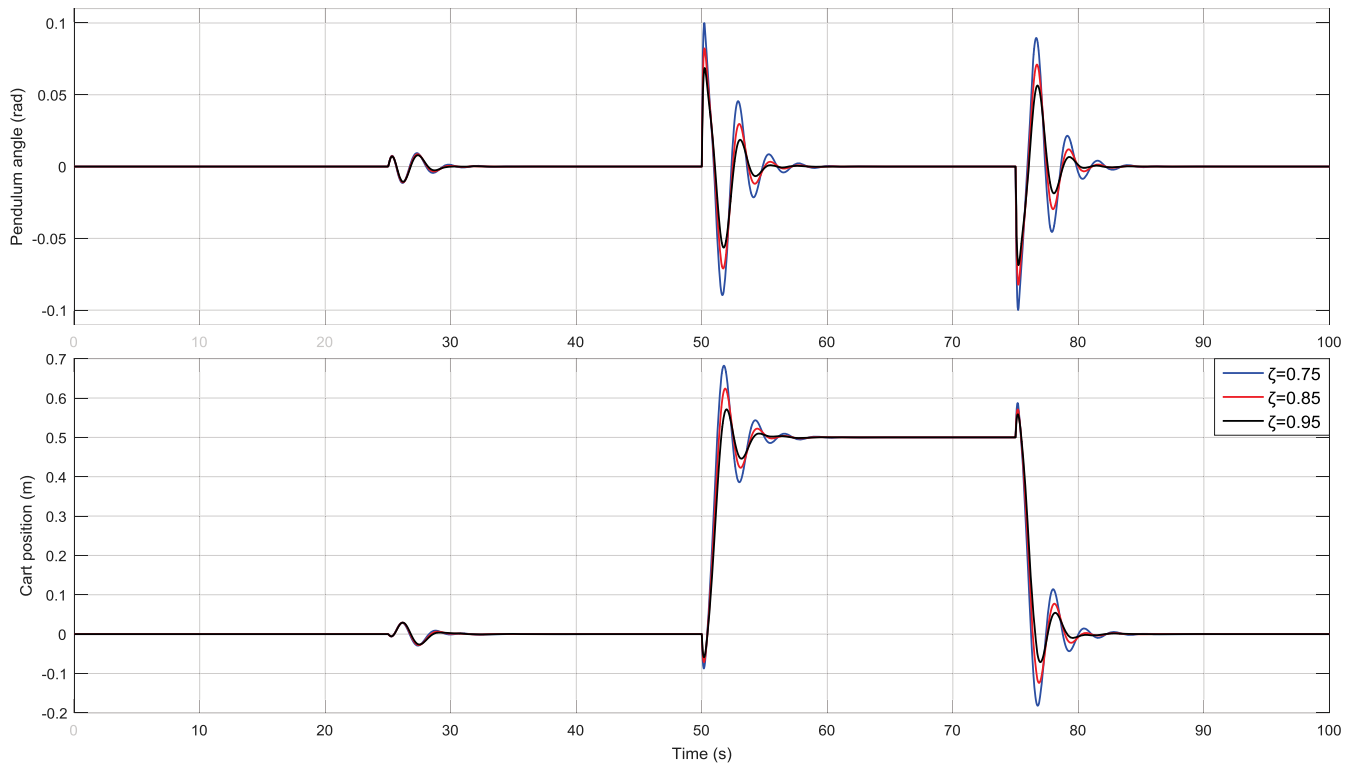


Figure 6. Responses for changing values of damping ratio ζ

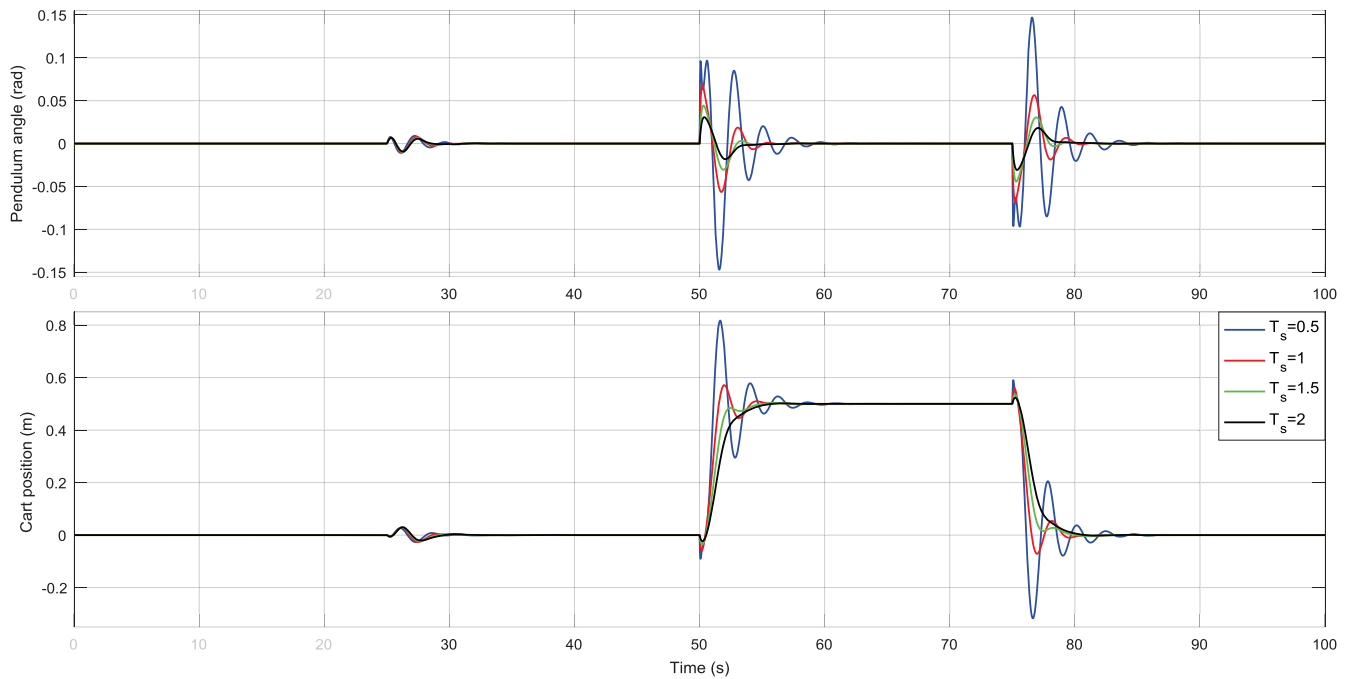


Figure 7. Responses for changing values of settling time T_s

V. CONCLUSION

An improved cascade control approach based on controller synthesis method is introduced in the paper to control a cart inverted pendulum system. Inner process is unstable and outer has double integrators. So, two PD blocks are used to make them stable before designing controllers. It is shown that the cart inverted pendulum system can be controlled effectively by adjusting only three parameters, one of which for inner loop and the others for outer loop. Real time implementation of the given approach can be considered as a future work.

ACKNOWLEDGMENT

This work is supported by Dicle University Coordinatorship of Scientific Research Projects (DUBAP) under grant no: 10-MF-44

REFERENCES

- [1] Y. Liu and H. Yu, "A survey of underactuated mechanical systems," *IET Control Theory Appl.*, vol. 7, no. 7, pp. 921–935, 2013.
- [2] A. N. K. Nasir, "Modeling and controller design for an inverted pendulum system," Universiti Teknologi Malaysia, 2007.
- [3] K. Razzaghi and A. A. Jalali, "A New Approach on Stabilization Control of an Inverted Pendulum, Using PID Controller," *Adv. Mater. Res.*, vol. 403, pp. 4674–4680, Nov. 2012.
- [4] P. Jaiwat and T. Ohtsuka, "Real-Time Swing-up of Double Inverted Pendulum by Nonlinear Model Predictive Control," in *5th International Symposium on Advanced Control of Industrial Processes*, 2014, pp. 290–295.
- [5] K. J. Åström and K. Furuta, "Swinging up a pendulum by energy control," *Automatica*, vol. 36, no. 2, pp. 287–295, Feb. 2000.
- [6] S. D. Hanwate and Y. V. Hote, "Design of PID controller for inverted pendulum using stability boundary locus," in *2014 Annual IEEE India Conference (INDICON)*, 2014, pp. 1–6.
- [7] A. Jacknoon and M. A. Abido, "Ant Colony based LQR and PID tuned parameters for controlling Inverted Pendulum," in *2017 International Conference on Communication, Control, Computing and Electronics Engineering (ICCCCEE)*, 2017, pp. 1–8.
- [8] S. K. Mishra and D. Chandra, "Stabilization and Tracking Control of Inverted Pendulum Using Fractional Order PID Controllers," *J. Eng.*, vol. 2014, pp. 1–9, 2014.
- [9] B. A. Elsayed, M. A. Hassan, and S. Mekhilef, "Fuzzy swinging-up with sliding mode control for third order cart-inverted pendulum system," *Int. J. Control. Autom. Syst.*, vol. 13, no. 1, pp. 238–248, Feb. 2015.
- [10] S. Mahjoub, F. Mnif, and N. Derbel, "Second-order sliding mode control applied to inverted pendulum," in *14th International Conference on Sciences and Techniques of Automatic Control & Computer Engineering - STA'2013*, 2013, pp. 269–273.
- [11] S. Rudra and R. K. Barai, "Robust Adaptive Backstepping Control of Inverted Pendulum on Cart System," *Int. J. Control Autom.*, vol. 5, no. 1, pp. 13–26, 2012.
- [12] X. Jia, Y. Dai, and Z. A. Memon, "Adaptive Neuro-fuzzy Inference System Design of Inverted Pendulum System on an Inclined Rail," in *2010 Second WRI Global Congress on Intelligent Systems*, 2010, vol. 3, pp. 137–141.
- [13] A. K. Singh and P. Gaur, "Adaptive control for non-linear systems using artificial neural network and its application applied on inverted pendulum," in *2010 India International Conference on Power Electronics (IICPE)*, 2011, pp. 1–8.
- [14] A. M. El-Nagar, M. El-Bardini, and N. M. El-Rabaie, "Intelligent control for nonlinear inverted pendulum based on interval type-2 fuzzy PD controller," *Alexandria Eng. J.*, vol. 53, no. 1, pp. 23–32, Mar. 2014.
- [15] I. Kaya and M. Nalbantoglu, "Cascade controller design using controller synthesis," in *2015 19th International Conference on System Theory, Control and Computing (ICSTCC)*, 2015, pp. 32–36.
- [16] Feedback Instruments Ltd., "Digital pendulum control experiments manual," Crowborough, 1160–33936S, 2010.